

## **Supplementary Materials**

### **Online Methods**

#### **Computational prediction of miRNA target genes and cis-acting elements for transcription factors.**

We used seven established miRNA target prediction algorithms: DIANA-microT3.1, miRanada, MirTarget2, PicTar, PITA, microcosm, and TargetScan5.1. Only the miRNAs that were predicted to target *KCNJ2* gene by at least four of the seven algorithms were considered as candidates for further analysis (1).

The binding sites for various transcription factors in the promoter regions of the host genes of miR-26a-1, miR-26a-2 and miR-26b from different species (human, canine, rat and mouse) were analyzed with *MatInspector* V2.2 (Genomatix) (2).

Analyses were made to the 5' flanking regions 5 kb upstream of the transcriptional start sites of the host genes (Supplemental Table 4).

#### **Bioinformatic identification of miR-26 as a candidate *KCNJ2*-regulating microRNA of interest.**

We first performed an initial miRNA screening microarray analysis of AF samples (described in one of our previous publications (3)) followed by a bioinformatic search for miRNAs that target *KCNJ2*. Initially, we suspected miR-101 as the primary candidate miRNA for *KCNJ2* regulation. However, in followup experiments, we found that the expression-levels of miR-101 in the human heart are very low compared to miR-1 or miR-26a/b (Figure A below), which makes miR-101 unlikely to be the principal regulator of *KCNJ2*. Therefore, we changed our strategy

and measured the expression levels of all the highly-conserved potential *KCNJ2*-targeting miRNAs in our atrial-tachypaced (ATP) dog samples, including miR-1, miR-16, miR-24, miR26a/b, miR-101 and miR-195, as shown in Figure B. After this screening, we selected miR-26a/b for study, based on the fact that it is the only microRNA that both targets *KCNJ2* and is highly expressed in the heart, with an expression-level that is downregulated in AF-models like the ATP dog.

Figure A

Relative expression of miR-26 and miR-101 in human LA

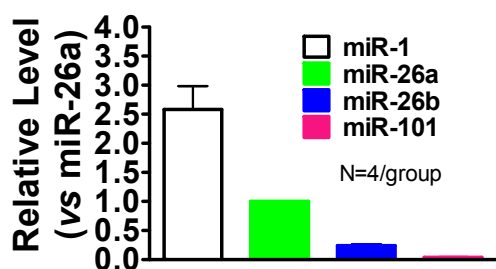
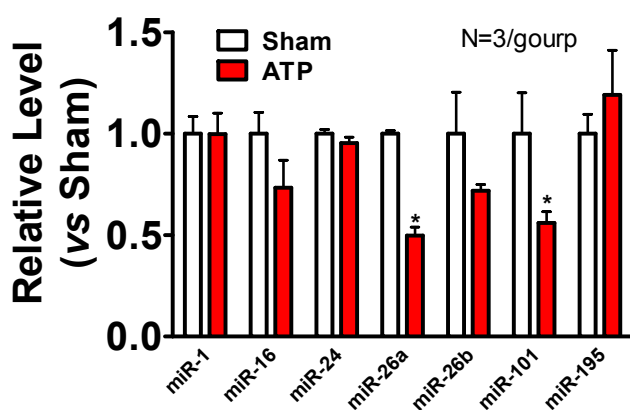


Figure B

Expression of *KCNJ2*-targeted miRNAs in atrium of ATP dogs



**Rapid amplification of cDNA ends (5'-RACE).** The transcription start sites (TSS) of the host genes *Ctdsp1* (for miR-26a-1), *Ctdsp2* (for miR-26a-2) and *Ctdsp1* (for miR-26b) were determined with Marathon cDNA Amplification Kit, as previously described (2, 4). Human RNA sample was purchased from Clontech (Mountain View, CA). The gene-specific primers (GSPs) used for PCR-amplification of miR-26 promoter sequences spanning NFAT *cis*-elements for chromatin immunoprecipitation assay (ChIP) are shown in Supplemental Table 5 and those for 5'RACE are shown in Supplemental Table 6.

**Verification of miR-Mask and miR-Mimic specificity.** Searches for complementarity of the sequences of miR-Mimic and miR-Masks to other functionally-known transcripts in the mouse genome were performed by BLAST to confirm the specificity for the *KCNJ2* gene. No significant complementarity was found to any other transcript with known function. The effectiveness and specificity of miR-Mask and miR-Mimic constructs was tested by assessing their ability to prevent and mimic (respectively) the effects of miR-26 on Kir2.1-expression and AF-vulnerability, as well as a lack of effect on miR-26 targets (cyclin D2 and E2) documented in the literature (5) as well as in the present study.

**Data analysis.** Group data are expressed as mean  $\pm$  SEM. Two-group only comparisons were performed by unpaired Student's *t*-test. Multiple-group comparisons for real-time RT-PCT and western blot experiments were analyzed by one-way ANOVA with Bonferroni -adjusted post-hoc *t*-tests. Differences in AF incidence were analyzed using  $\chi^2$ -test. To account for multiple testing, we selected for comparison only results of primary biological significance and

applied a correction using the Holm-Bonferroni method. The statistical significances of multiple-group comparisons for AF duration were obtained with one-way ANOVA on all data, followed by post-hoc Tukey tests. A two-tailed  $p < 0.05$  was taken to indicate a statistically significant difference.

### Online References

1. Luo X, Zhang H, Xiao J, Wang Z. Regulation of human cardiac ion channel genes by microRNAs: Theoretical perspective and pathophysiological implications. *Cell. Physiol. Biochem.* 2010;25:571-586.
2. Lin H, Xiao J, Luo X, Pan Z, Yang B, Wang Z. Transcriptional control of pacemaker channel genes *HCN2* and *HCN4* by Sp1 and implications in re-expression of these genes in hypertrophic heart. *Cell. Physiol. Biochem.* 2009;23:317-326.
3. Lu Y, et al. MicroRNA-328 contributes to adverse electrical remodeling in atrial fibrillation. *Circulation* 2010;122:2378-2387.
4. Luo X, Xiao J, Lin H, Lu Y, Yang B, Wang Z. Genomic structure, transcriptional control and tissue distribution of human *ERG1* and *KCNQ1* genes. *Am. J. Physiol.* 2007;294:H1371-H1380.
5. Kota J, et al. Therapeutic microRNA delivery suppresses tumorigenesis in a murine liver cancer model. *Cell.* 2009;137:1005-1017.

### Supplemental Figure Legends

**Supplemental Figure 1.** Alignment of sequences of mature miR-26 family miRNAs of different species. The sequences of miR-26a-1 and miR-26a-2 are identical among species. The seed sites (5' end 2-8 nucleotides) are highlighted in yellow. Note that the human sequences of miR-26a and miR-26b are identical to mouse (and other species as well), which justifies the use of these miRNAs in mouse experiments.

**Supplemental Figure 2.** Sequences of miR-26a/b and their antisense molecules used in our study. **(a)** Alignment of the sequences of miR-26a/b (upper sequences) with their target sites in the 3'-UTRs of human *KCNJ2* (lower sequences). The complementarity is indicated by boldface letters highlighted in yellow and connected by “|”. **(b)** Sequences of the negative control miRNA (miR-NC) and negative control miRNA antisense oligodeoxynucleotides (AMO-NC).

**Supplemental Figure 3.** Western blot analysis of the effects of miR-26 on protein levels of several K<sup>+</sup> channel pore-forming  $\alpha$ -subunits. **(a)** Lack of effect of miR-26a on human *ether-ago-go*-related gene (HERG) K<sup>+</sup> channel subunit responsible for the rapid delayed-rectifier K<sup>+</sup> current ( $I_{Kr}$ ). +AMO-26a: co-transfection of miR-26a and AMO-26a; miR-NC: negative control miRNA; AMO-NC: negative control AMO. **(b)** Lack of effect of miR-26a on human voltage-gated long QT K<sup>+</sup> channel subunit 1 (KvLQT1) responsible for the slow delayed-rectifier K<sup>+</sup> current ( $I_{Ks}$ ). **(c)** Lack of effect of miR-26a on human voltage-gated shaker-type of K<sup>+</sup> channel subunit (Kv4.3) responsible for the transient outward K<sup>+</sup> current ( $I_{to1}$ ). n=3/group.

**Supplemental Figure 4.** Sequences of the antisense to miR-26a **(a)** with locked nucleotides (LNA-antimiR-26a) and the mismatched LNA-antimiR-26a (MM

LNA-antimiR-26a) for negative control. The complementarity between LNA-antimiR-26a or MM LNA-antimiR-26a and miR-26a/b is highlighted in yellow. The boldface and underlined letters represent the LNA-modified nucleotides. The lower case letters indicate the mismatched nucleotides. Note that the miRNA sequence of miR-26a is 100% conserved among human, rat and mouse.

**Supplemental Figure 5.** Schematic illustration of construction of adenovirus vector carrying mouse pre-miR-26a-1. Mouse miR-26a-1 precursor DNA (5'-GGATCCg TTCCGGCACCGGAGCAAGTTCATTAGGTCCTATCCGACACGTCCAGGGTTCC CCGGATAAGAACCAATGAACGTGCCCTGCGCCCGGACtttttAAGCTT-3') was inserted into adenovirus shuttle plasmid pDC316-EGFP-U6. pDC316-EGFP-U6 was then co-transfected with the infectious adenovirus genomic plasmid pBHGlox $\Delta$ E1,3Cre into 293 cells by lipofectamine. Following co-transfection of these two DNAs, homologous recombination occurred to generate a recombinant adenovirus in which pre-miR-26a-1 is incorporated into the viral genome, replacing the  $\Delta$ E1 region. The control vector (Adv-miR-free) lacked the pre-miR-26a DNA unit.

**Supplemental Figure 6.** One contemporaneous set of wild type controls was performed for all groups. For clarity, results are shown separately for different sets of interventions in Figures 3 and 4 of the main manuscript. However, statistical comparisons were performed considering all groups simultaneously, as shown in this figure. AF incidence comparisons (a) were by  $\chi^2$ , with correction for multiple testing by the Holm-Bonferroni method. AF durations (b) were compared by one-way ANOVA with post-hoc Tukey's tests.

**Supplemental Figure 7.** Verification of cellular uptake of Adv-miR-26a-1 in mouse atrial tissues. Adv-miR-26a-1 was administered by direct injection into tail veins. Three days after Adv-miR-26a-1 administration, the animals were scarified and atrial tissues were sliced for laser scanning confocal microscope examination. Cardiomyocytes stained in green (GFP incorporated in the viral vector) indicate successful Adv-miR-26a-1 uptake. Control samples were obtained from sham-operated, age-matched mice. The images shown are from three independent experiments from three separate animals from each group.

**Supplemental Figure 8.** Verification of the ability of the LNA-antimiR-26a to upregulate (**A**), and adv-miR-26a to downregulate (**B**), atrial Kir2.1 protein level in mice, determined by Western blot analysis with protein samples from atrial tissues. Their respective negative control constructs were also examined.  $*p<0.05$ ,  $**p<0.01$  vs Ctl; n=6 for each group. **C and D.** Verification of Adv-miR-26a on two proven targets of miR-26, Cyclin D2 and Cyclin E2 (**5**).  $**p<0.01$  vs WT; n=5/group. The LNA constructs were injected into mice via tail vein at a dosage of 5 mg/kg/day in 0.2 ml saline once a day for three consecutive days, and Adv constructs were injected through the tail vein at  $10^{10}$  pfu/ml in 100  $\mu$ l. The atrial tissues for the analyses were obtained 3 days after the last construct administration.

**Supplemental Figure 9.** Sequences of the miR-Mimic (**a**) and miR-Mask (**b**) and their mismatched counterparts as negative control constructs used in our study. The complementarity between the guide strand of the miR-Mimic or miR-Mask and the 3'UTR of KCNJ2 is highlighted in yellow and connected by “|”. The boldface and underlined letters represent the LNA-modified nucleotides. The lower case letters

indicate the mismatched nucleotides to *KCNJ2*. GS: guide strand; PS: passenger strand. The two miR-Masks were designed to fully base pair the two binding sites for miR-26 in the 3'UTR of *KCNJ2* so as to protect these sites from binding miR-26. Searches for complementarity of the sequences of miR-Mimic and miR-Masks to other functionally-known transcripts in the mouse genome were performed by BLAST to confirm the specificity for the *KCNJ2* gene.

**Supplemental Figure 10.** Identification of transcription start sites (TSSs) and genomic characteristics of the host genes of the miR-26 family miRNAs using 5'RACE techniques. **(a)** DNA gel image showing the single, discrete bands obtained by 5'RACE, indicating a single TSS for each host gene (*Ctdsp2*, *Ctdspl* or *Ctdsp1*). **(b)-(d)** Genomic sequences of *Ctdspl* for miR-26a-1, *Ctdsp2* for miR-26a-2, and *Ctdsp1* for miR-26b. TSSs are indicated; putative NFAT binding sites are shown in red letters; the fragments highlighted in green containing NFAT binding sites are those used for promoter activity analysis by luciferase assay. The outer and inner (nested) primers for 5'RACE, and the forward and reverse primers for ChIP experiments, are indicated by lines above or below the sequences.

**Supplemental Figure 11.** The constructs used to inhibit the function of nuclear factor of activated T-cells (NFAT). **(a)** Sequences of decoy oligodeoxynucleotide (dODN) fragments used to sequester NFAT (dODN-NFAT) and the negative control dODN (dODN-NC). **(b)** Sequences of small interference RNA (siRNA) used to knock down the cardiac isoforms of NFAT: NFATc3 and NFATc4.

**Supplemental Figure 12.** Verification of the efficacy of siRNAs in knocking down the cardiac isoforms of NFAT, NFATc3 and NFATc4, assessed by qPCR **(a)** and by

Western blot analysis (**b**) in H9c2 rat ventricular cells. siRNA to NFATc3 and siRNA to NFATc4 were co-transfected into cells. NC: negative control siRNA.  $**p<0.01$ ,  $***p<0.001$  vs Ctl; n=4 for each group.

**Supplemental Figure 13.** Effects of NFAT inhibition on expression of miR-1, determined by qPCR in H9c2 rat ventricular cells. Control cells were mock-treated with lipofectamine 2000 for experiments involving transfection of dODN-NFAT or siRNAs. Note that NFAT does not affect miR-1 level. n=3 for INCA group and n=4 for the other groups.

**Supplemental Figure 14.** **A.** AF incidence in 1-week and 6-week atrial tachypacing (ATP) canine model. **B.** AF duration in ATP canine model. **C.** Quantitative RT-PCR measurement of miR-26a in atrium and ventricle of 1-wk and 6-wk ATP dogs. **D.** Western blot analysis of Kir2.1 protein in atrium and ventricle of 1-wk and 6-wk ATP dogs. n=5/group;  $*p<0.05$ ,  $**p<0.01$ ,  $***p<0.001$ .

## Supplemental Figures

### Supplemental Figure 1

	miR-26a-1/miR-26a-2	miR-26b
Human	U <b>UCAAGUA</b> AUCCAGGAUAGGCU-3'	U <b>UCAAGUA</b> AUUCAGGAUAGGU-3'
Canine	U <b>UCAAGUA</b> AUCCAGGAUAGGCU-3'	U <b>UCAAGUA</b> AUUCAGGAUAGGUU-3'
Rat	U <b>UCAAGUA</b> AUCCAGGAUAGGCU-3'	U <b>UCAAGUA</b> AUUCAGGAUAGGU-3'
Mouse	U <b>UCAAGUA</b> AUCCAGGAUAGGCU-3'	U <b>UCAAGUA</b> AUUCAGGAUAGGU-3'

**Supplemental Figure 1.** Alignment of sequences of mature miR-26 family miRNAs of different species. The sequences of miR-26a-1 and miR-26a-2 are identical among species. The seed sites (5'end 2-8 nucleotides) are highlighted in yellow. Note that the human sequences of miR-26a and miR-26b are identical to mouse (and other species as well), which justifies the use of these miRNAs in mouse experiments.

## Supplemental Figure 2

**a. miR-26:KCNJ2 Complementarity****miR-26a**

```

3'-UCCGGAUAGGACCUAAUGAACUU-5'
   |::| | | | | | | |
254-UGUUUUUCC---AAAACUUGAA-272
254-UGUUUUUCC---AAActgctgA-272

```

miR-26a

3'UTR of KCNJ2 (Binding Site 1)  
Mutant 3'UTR of KCNJ2

```

3'-UCGGAUAGGACCUAAUGAACUU-5'
   | | | | | | | |
3132-UCCCUCUAAGAGGUAUACUUGAA-3153
3132-UCCCUCUAAGAGGUAUctgctgA-3153

```

miR-26a

3'UTR of KCNJ2 (Binding Site 2)  
Mutant 3'UTR of KCNJ2**miR-26b**

```

3'-UGGAUAGGACCUAAUGAACUU-5'
   |::| | | | | | | |
255-GUUUUUCC---AAAACUUGAA-272
255-GUUUUUCC---AAActgctgA-272

```

miR-26b

3'UTR of KCNJ2 (Binding Site 1)  
Mutant 3'UTR of KCNJ2

```

3'-UGGAUAGGACUAAAUGAACUU-5'
   | | | | | | | |
3133-CCCUCUAAGAGGUAUACUUGAA-3153
3133-CCCUCUAAGAGGUAUctgctgA-3153

```

miR-26b

3'UTR of KCNJ2 (Binding Site 2)  
Mutant 3'UTR of KCNJ2**b. Negative Control miRNA and AMO miR-NC****miR-NC**

```

5'-UCAUAAAGCUGAUACCUCUAGAU-3'
3'-UAAGUAUUUCGACUAUUGGAGAUC-5'

```

**AMO-NC**

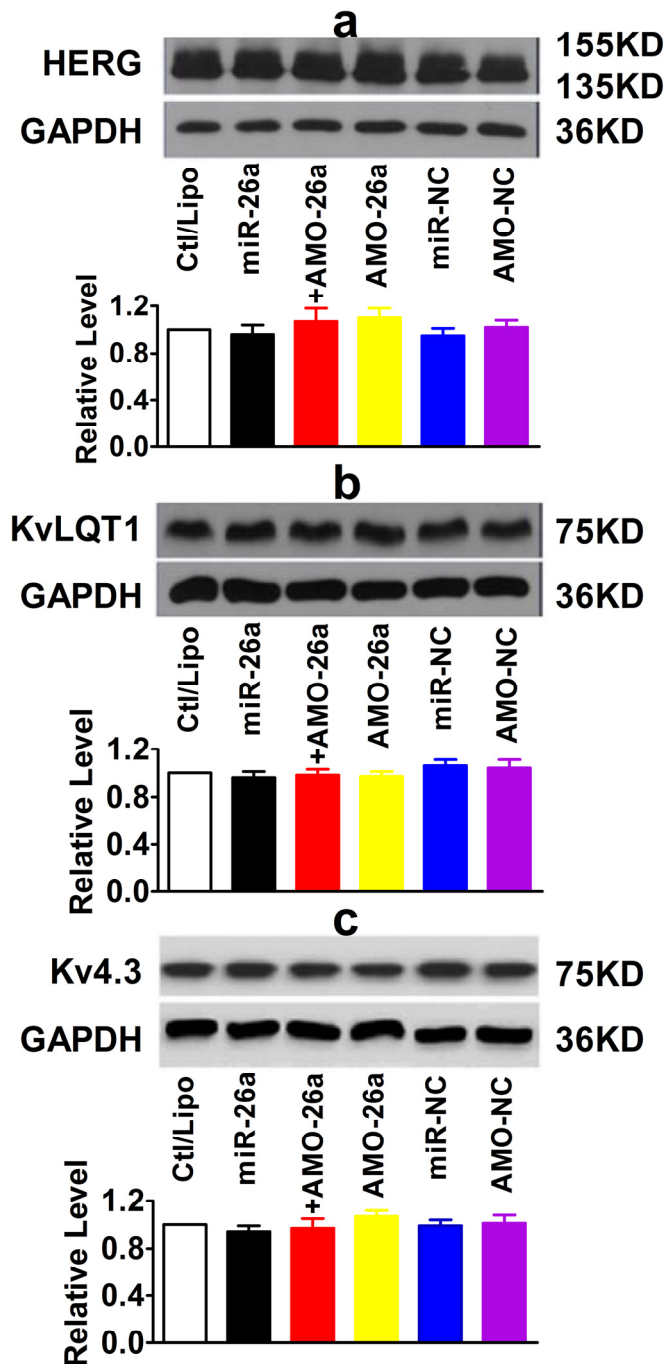
```

5'-TCATACAGCTAGATAACCAAAGA-3'

```

**Supplemental Figure 2.** Sequences of miR-26a/b and their antisense molecules used in our study. **(a)** Alignment of the sequences of miR-26a/b (upper sequences) with their target sites in the 3'-UTRs of human *KCNJ2* (lower sequences). The complementarity is indicated by boldface letters highlighted in yellow and connected by “|”. **(b)** Sequences of the negative control miRNA (miR-NC) and negative control miRNA antisense oligodeoxynucleotides (AMO-NC).

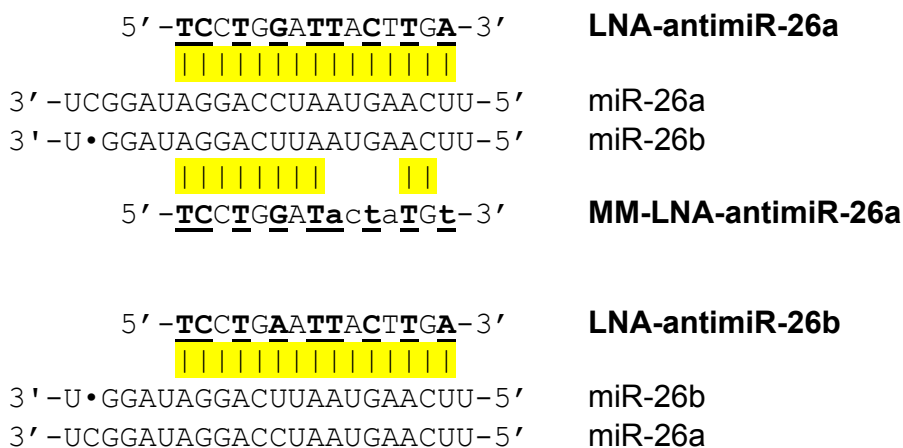
## Supplemental Figure 3



## Supplemental Figure 3.

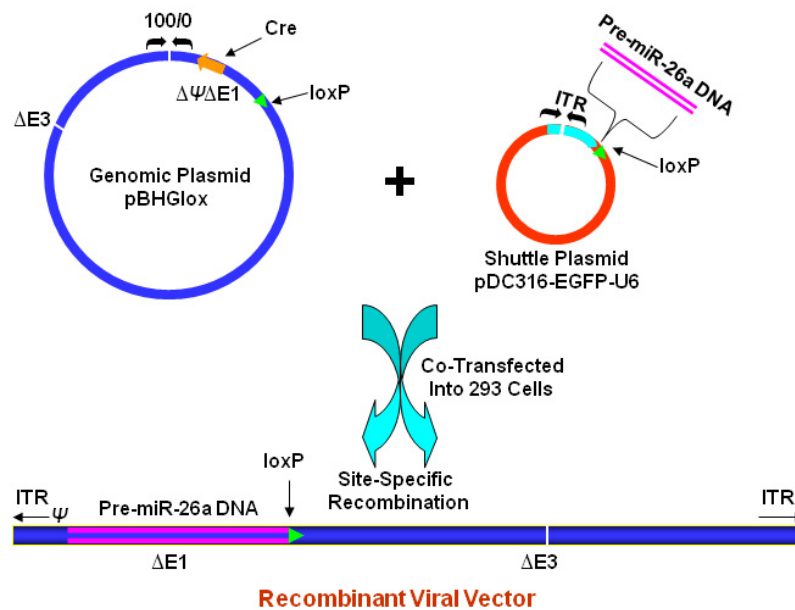
Western blot analysis of the effects of miR-26 on protein levels of several K<sup>+</sup> channel pore-forming  $\alpha$ -subunits. (a) Lack of effect of miR-26a on human *ether-ago-go*-related gene responsible for the rapid delayed-rectifier K<sup>+</sup> current ( $I_{Kr}$ ). +AMO-26a: co-transfection of miR-26a and AMO-26a; miR-NC: negative control miRNA; AMO-NC: negative control AMO. (b) Lack of effect of miR-26a on human voltage-gated long QT K<sup>+</sup> channel subunit 1 (KvLQT1) responsible for the slow delayed-rectifier K<sup>+</sup> current ( $I_{Ks}$ ). (c) Lack of effect of miR-26a on human voltage-gated shaker-type of K<sup>+</sup> channel subunit (Kv4.3) responsible for the transient outward K<sup>+</sup> current ( $I_{to1}$ ). n=3/group.

## Supplemental Figure 4



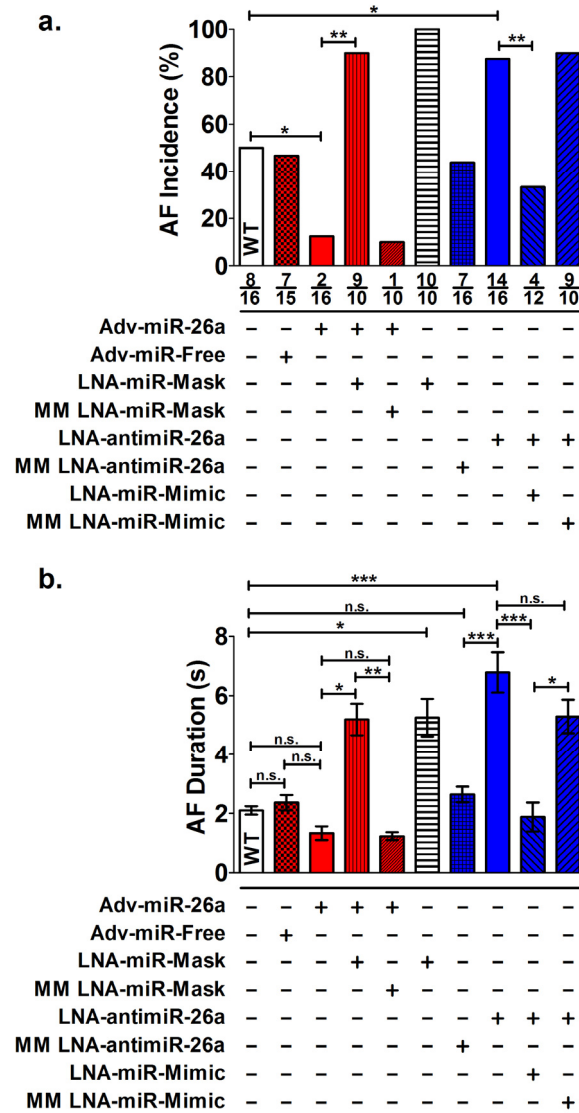
**Supplemental Figure 4.** Sequences of the antisense to miR-26a (a) with locked nucleotides (LNA-antimiR-26a) and the mismatched LNA-antimiR-26a (MM LNA-antimiR-26a) for negative control. The complementarity between LNA-antimiR-26a or MM LNA-antimiR-26a and miR-26a/b is highlighted in yellow. The boldface and underlined letters represent the LNA-modified nucleotides. The lower case letters indicate the mismatched nucleotides. Note that the miRNA sequence of miR-26a is 100% conserved among human, rat and mouse.

## Supplemental Figure 5



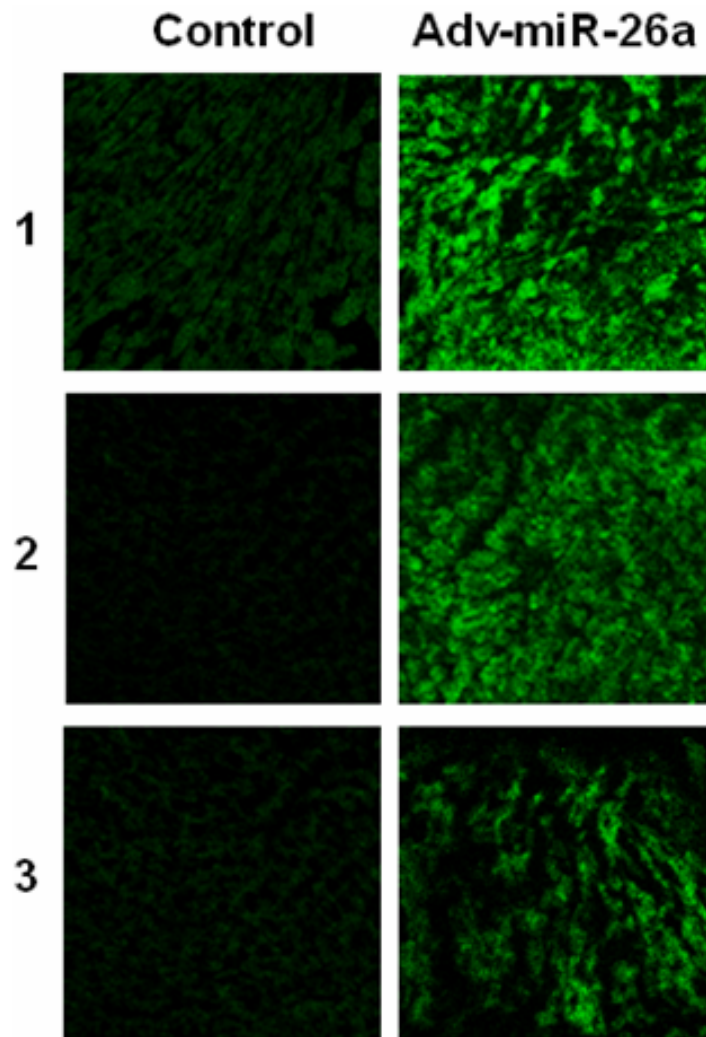
**Supplemental Figure 5.** Schematic illustration of construction of adenovirus vector carrying mouse pre-miR-26a-1. Mouse miR-26a-1 precursor DNA (5'-GGATCCg TTCCGGCACCGGAGCAAGTTCATTAGGTCCTATCCGACACGTCCAGGGTCCCCGG ATAAGAACCAATGAACGTGCCCTGCGCCCGGACtttttAAGCTT-3') was inserted into adenovirus shuttle plasmid pDC316-EGFP-U6. pDC316-EGFP-U6 was then co-transfected with the infectious adenovirus genomic plasmid pBHGlox $\Delta E1,3$ Cre into 293 cells by lipofectamine. Following co-transfection of these two DNAs, homologous recombination occurred to generate a recombinant adenovirus in which pre-miR-26a-1 is incorporated into the viral genome, replacing the  $\Delta E1$  region. The control vector (Adv-miR-free) lacked the pre-miR-26a DNA unit.

Supplemental Figure 6



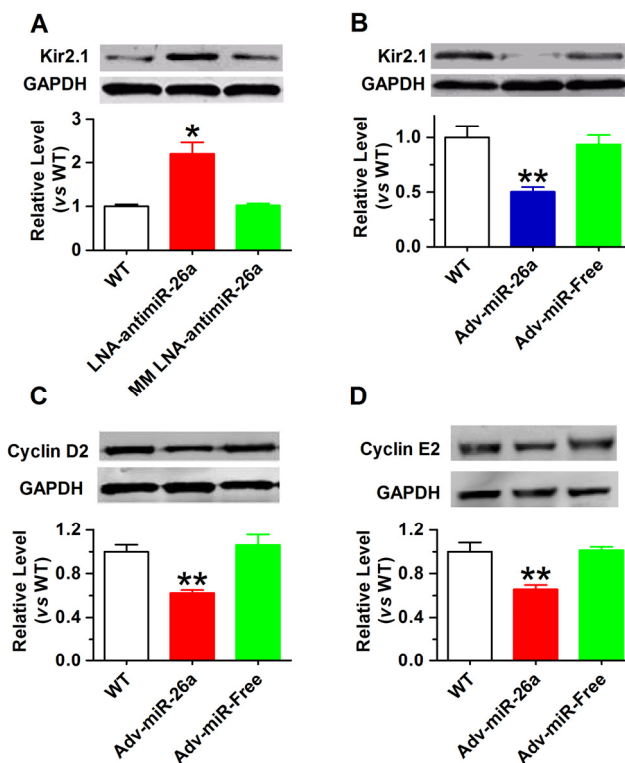
**Supplemental Figure 6.** One contemporaneous set of wild type controls was performed for all groups. For clarity, results are shown separately for different sets of interventions in Figures 3 and 4 of the main manuscript. However, statistical comparisons were performed considering all groups simultaneously, as shown in this figure. AF incidence comparisons (a) were by  $\chi^2$ , with correction for multiple testing by the Holm-Bonferroni method. AF durations (b) were compared by one-way ANOVA with post-hoc Tukey's tests.

Supplemental Figure 7



**Supplemental Figure 7.** Verification of cellular uptake of Adv-miR-26a-1 in mouse atrial tissues. Adv-miR-26a-1 was administered by direct injection into tail veins. Three days after Adv-miR-26a-1 administration, the animals were sacrificed and atrial tissues were sliced for laser scanning confocal microscope examination. Cardiomyocytes stained in green (GFP incorporated in the viral vector) indicate successful Adv-miR-26a-1 uptake. Control samples were obtained from sham-operated, age-matched mice. The images shown are from three independent experiments from three separate animals from each group.

## Supplemental Figure 8

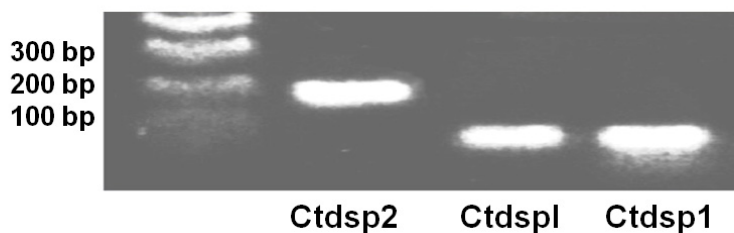


**Supplemental Figure 8.** Verification of the ability of the LNA-antimiR-26a to upregulate (A), and adv-miR-26a to downregulate (B), atrial Kir2.1 protein level in mice, determined by Western blot analysis with protein samples from atrial tissues. Their respective negative control constructs were also examined. \* $p < 0.05$ , \*\* $p < 0.01$  vs Ctl;  $n = 6$  for each group. C and D. Verification of Adv-miR-26a on two proven targets of miR-26, Cyclin D2 and Cyclin E2 (5). \*\* $p < 0.01$  vs WT;  $n = 5$ /group. The LNA constructs were injected into mice via tail vein at a dosage of 5 mg/kg/day in 0.2 ml saline once a day for three consecutive days, and Adv constructs were injected through the tail vein at  $10^{10}$  pfu/ml in 100  $\mu$ l. The atrial tissues for the analyses were obtained 3 days after construct administration.



### Supplemental Figure 10

#### a. DNA gel



**Supplemental Figure 10.** Identification of transcription start sites (TSSs) and genomic characteristics of the human host genes of the miR-26 family miRNAs using 5'RACE techniques. (a) DNA gel image showing the single, discrete bands obtained by 5'RACE, indicating a single TSS for each host gene (Ctdsp2, Ctdsp1 or Ctdsp1). (b)-(d) See below. Genomic sequences of Ctdsp1 for miR-26a-1, Ctdsp2 for miR-26a-2, and Ctdsp1 for miR-26b. TSSs are indicated; putative NFAT binding sites are shown in red letters; the fragments highlighted in green containing NFAT binding sites are those used for promoter activity analysis by luciferase assay. The outer and inner (nested) primers for 5'RACE, and the forward and reverse primers for ChIP experiments, are indicated by lines above or below the sequences.

## Supplemental Figure 10

**b. Ctdspl/miR-26a-1**

-3626 CAACTCCCTA CTTGTCATTT TAGATAACTC TGAGATCCCC AGTGTCTAGA  
 -3576 GCAGAACCTT GCATATAGAA TATGCACTCA ATAAATGTTT GTTGAATGAA

**Forward Primer**

-3526 TATAGCCAAA TTTATCAGTC TTATCCTGGC AATTTCTTAA GTTTTTGTCA

**/ChIP**

-3476 CTCTCAGGCC TTTCCCATCC AAGATCAAAA AGCACTTACC CATTGTCTCT  
 -3426 GGTATATGTT AATTTTTTAT ATTTAATTAT TCAGTCTATC TTGAATGTGC

**Reverse Primer/ChIP**

-3376 TGTAAGGACT GGGATAAAGA TATATTTTTT CCTCATGGAT AGGTACTTGT

**NFAT Binding Site**

-3326 CCCAACAATT TTTGATCTT TCTTTCATGT GTAAAACCAA AATACTGTGT  
 -3276 TATCTAAGAC TGTTTCAGTA AGGTATTATG CAATCACTTA TAATAGTAGT  
 -3226 AACAGCAATT ATGTCACCAC ATAAGAAAAT GCTAACCTTA TAATTTTTAA  
 -3176 CATGGCTTTT TTATAGCTAC ATAAAATTAT GTCAGCATAT AGGCAAGGAC

.....  
 .....  
 .....  
 -676 TGCCTCAGAC TCCTCCCCAC ATCTCTCACA CCCCAGGCCT CTCACCTCAC  
 -626 TCATTCTGCC AGGCCCCCTT GACACCCCTC ACTTCTAACC CCCCAGGCC  
 -576 CTCTGCCGTC CGCTACACCC CGAGCCCCTC ACCCCACTCA ACTGCCCCGG  
 -526 GCCCCCGCGC GCGCGGCCGC CCCCTCCCGC CCTCCACTCA CCCTGTGTCG

**→TSS (+1)**

-26 GGGGGGCCGG GCCTGCGGGC GGCCGC CGCGCACCC ATGGACGGCC  
 +25 CGGCCATCAT CACCCAGGTG ACCAACCCCA ATGGACGGCC CGGCCATCAT

**↳ Translation Start Site****Inner Primer/5'RACE**

+75 CACCCAGGTG ACCAACCCCA AGGAGGACGA GGGCCGGTTG C

**Outer Primer/5'RACE**

**Supplemental Figure 10b.** Identification of transcription start sites (TSSs) and genomic characteristics of the host genes of the miR-26 family miRNAs using 5'RACE techniques. Genomic sequences of Ctdspl for miR-26a-1. TSSs are indicated; putative NFAT binding sites are shown in red letters; the fragments highlighted in green containing NFAT binding sites are those used for promoter activity analysis by luciferase assay. The outer and inner (nested) primers for 5'RACE, and the forward and reverse primers for ChIP experiments, are indicated by lines above or below the sequences.

### Supplemental Figure 10

#### c. Ctdsp2/miR-26a-2

-3792 GGACACCCAG TCCGACTTCA GTAGCCACAG CAGGAGACAG ACAGGGACAG

#### Forward

-3742 CCACTCCATG TTTGCCCCAC ATAGCCCCC ATTCTAGCAT TTGGGGGTAA

#### Primer/ChIP

-3692 TGGGGACACT GCTGT **TGTTT CCAAATTGCC TCTTACCAAC CATGCAGTCA**  
 -3642 **GAGAGGCCAG AGGAAAGGG ATACA**GCAGG TAGGGAACCA AGTGAGAGTC

#### NFAT Binding Site

#### Reverse Primer/ChIP

-3592 **AGTC**GGCTTT CTCCTGGGAG AGTTGTTAGA CCTGGCTTCA GCTATCTCCC  
 -3542 TTGAACCACC TAAAATGAAC CACCTAAAGT TACACAACCA GCAACTGGCC

.....  
 .....  
 .....

#### ↗TSS (+1)

-42 TCGATTACTC ACTATAGGGC TCGAGCGGCC GCCCGGGCAG **GT****C**GCTTTTT  
 +8 CCGTAACAAA ATAGCAAAGC TCCCGACTGT CCGCAGCCCC GGCCGCTCAC  
 +58 AGATGGAGGG TCCAGGGCC TAGGACGCAG CCCCAGCGG GAAGCTCCAG

#### Inner Primer/5'RACE

+108 CTGGCCGTGA AGAGGCCGAG TCGAGAGCCG GGAGGCGCGC GGGGGTGGGC

#### Outer Primer/5'RACE

**Supplemental Figure 10c.** Identification of transcription start sites (TSSs) Genomic sequence of Ctdsp2 for miR-26a-2. TSSs are indicated; putative NFAT binding sites are shown in red letters; the fragments highlighted in green containing NFAT binding sites are those used for promoter activity analysis by luciferase assay. The outer and inner (nested) primers for 5'RACE, and the forward and reverse primers for ChIP experiments, are indicated by lines above or below the sequences.

## Supplemental Figure 10

## d. Ctdsp1/miR-26b

-542 ATTCAAGAGC GTGATTCTGA GGTTTGCACA GCTGTTTCGG GCCAGCAGAG

**Forward Primer/ChIP**

-492 CCTTCGCTGG CTCTTGACGT CCTTGCGAGG TGATCTCTGC GACCACCAGA

-442 CAGGAGAGAA GACCCATTTT ACAGATGAGG TAGTGCTATC TCCAAGTCCT

-392 CAACGAGGAA ACCGAGAAGC CTCTAGTCCC GGGTCTTCAG AAAACGCA GA

**NFAT Binding Site****Reverse Primer**

-342 GGTGGAGCCG CGCCGCACTC GGGCACTCCC CGGCGTGGGC GCTCCCGGCG  
**/ChIP**

-292 GCGGGCCCTT GGCCGAGGGC GCTCGGCGGC CTGGAACGGT GAGCCGGGTG

-242 CCGGGCCTGC CACGCAGCCG CAGAGACTCA GCCCCGCCGG CGGGCGGCAG

-192 GAAGGGAGGC GACGCCCCCT GGAGCGCGGC AGGAACCCGG CCCGGCCCCG

-142 CTCCCAGTCC CGCCTAGCCG CGCCGGTCCC AGAAGTGGCG AAAGCCGCAG

-92 CCGAGTCCAG GTCACGCCGA AGCCGTTGCC CTTTTAAGGG GGAGCCTTGA

-42 AACGGCGCCT GGGTTCCATG TTTGCATCCG CCTCGCGGGA AG**G**AAACTCC  
↗ **TSS (+1)**

**Inner Primer/5'RACE**

+9 ATGTTGTAAC AAAGTTTCCT CCGCGCCCCC TCCCTCCCCC TCCCCCCTAG

**Outer Primer/5'RACE**

+59 AACCTGGCTC CCCTCCCCTC CGGAGCTCGC GGGGATCCCT CCCTCCCACC

+109 CCTCCCCTCC CCCCCGCGCC CCGATTCCGG CCCCAGCCGG GGGGGAGGCC

+159 GGGCGCCCGG GCCAGAGTCC GGCCGGAGCG GAGCGCGCCC GGCCCC**ATG**G

**Translation Start Site**

+209 ACAGCTCGGC CGTCATTACT CAGATCAGCA AGGAGGAGGC TCGGGGCCCC

**Supplemental Figure 10d.** Identification of transcription start sites (TSSs) and genomic characteristics of the host genes of the miR-26 family miRNAs using 5'RACE techniques. **(d)** Genomic sequence of Ctdsp1 for miR-26b. TSSs are indicated; putative NFAT binding sites are shown in red letters; the fragments highlighted in green containing NFAT binding sites are those used for promoter activity analysis by luciferase assay. The outer and inner (nested) primers for 5'RACE, and the forward and reverse primers for ChIP experiments, are indicated by lines above or below the sequences.

## Supplemental Figure 11

### a. Decoy Oligodeoxynucleotides (dODN)

#### dODN-NFAT

5' -CGCCCAAAGA **GGAA** AATTTGTTTCATA-3'  
 3' -GCGGGTTTCTCCTTTTAAACAAAGTAT-5'

#### dODN-NC

5' -TAGTTATGCATCACGACCTGAT-3'  
 3' -ATCAATACGTAGTGCTGGACTA-5'

### b. Small Interfering RNA (siRNA)

#### siRNA-NFATc3

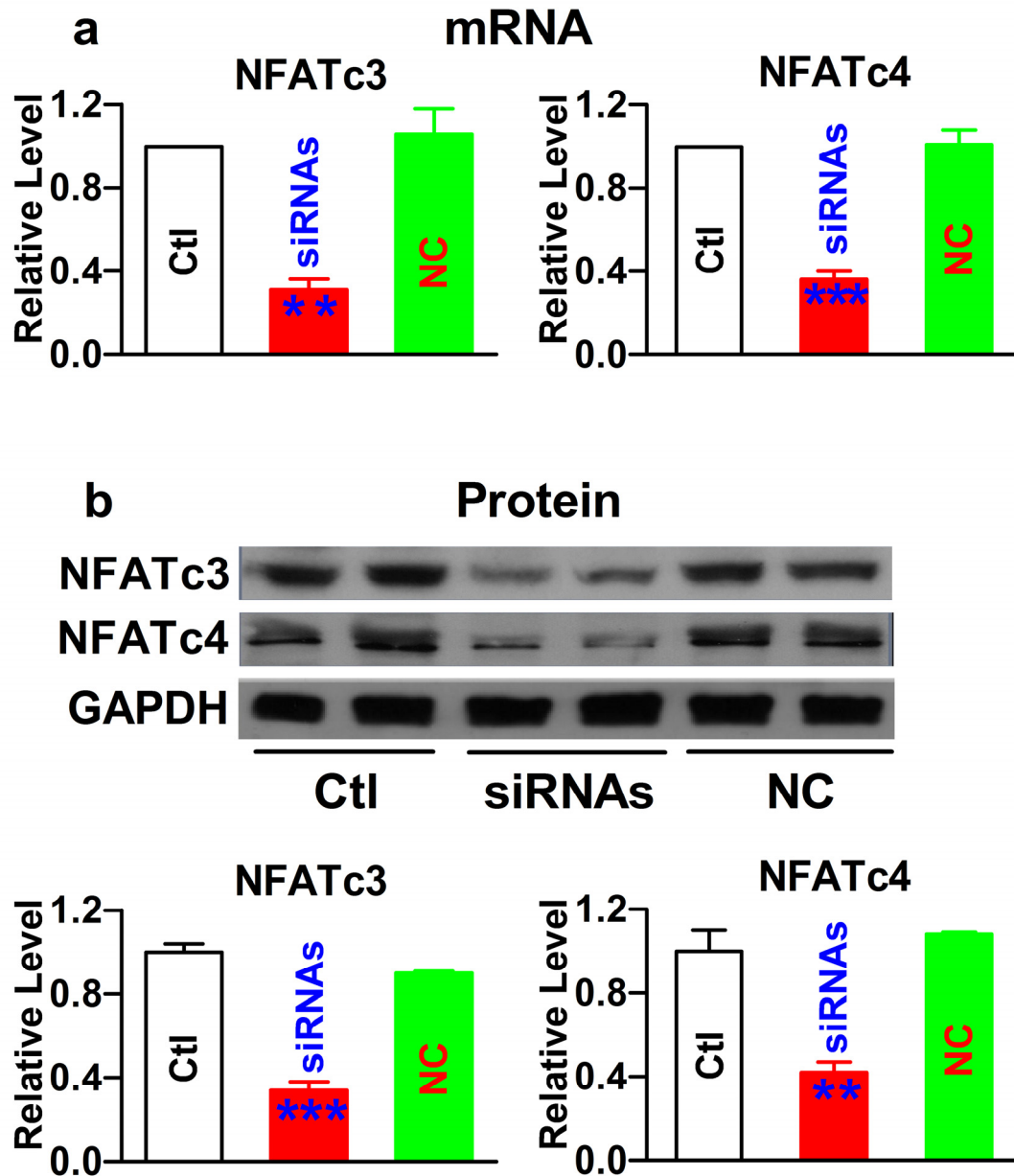
5' -UUAUCUCCCUUCUACCUCCACUG-3'  
 3' -AAUAGAAGGGAAGAUGGAGGGUGAC-5'

#### siRNA-NFATc4

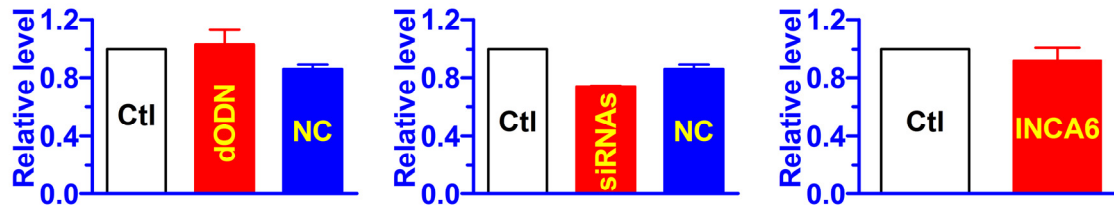
5' -ACCGAGUCACGAAUCUCCCAUCUAA-3'  
 3' -UGGCUCAGUGCUUAGAGGGUAGAUU-5'

**Supplemental Figure 11.** The constructs used to inhibit the function of nuclear factor of activated T-cells (NFAT). **(a)** Sequences of decoy oligodeoxynucleotide (dODN) fragments used to sequester NFAT (dODN-NFAT) and the negative control dODN (dODN-NC). **(b)** Sequences of small interference RNA (siRNA) used to knock down the cardiac isoforms of NFAT: NFATc3 and NFATc4.

Supplemental Figure 12

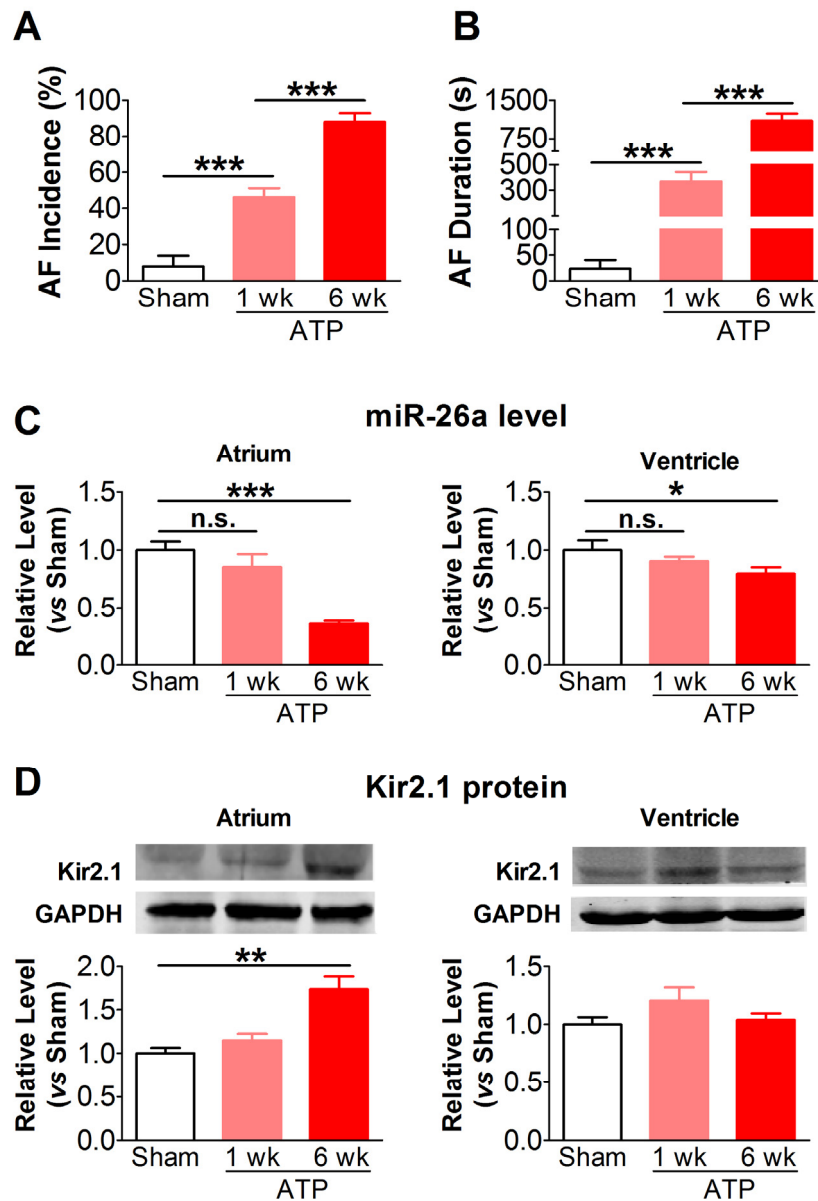


**Supplemental Figure 12.** Verification of the efficacy of siRNAs in knocking down the cardiac isoforms of NFAT, NFATc3 and NFATc4, assessed by qPCR (**a**) and by Western blot analysis (**b**) in H9c2 rat ventricular cells. siRNA to NFATc3 and siRNA to NFATc4 were co-transfected into cells. NC: negative control siRNA. \*\* $p < 0.01$ , \*\*\* $p < 0.001$  vs Ctl;  $n = 4$  for each group.

**Supplemental Figure 13**

**Supplemental Figure 13.** Effects of NFAT inhibition on expression of miR-1, determined by qPCR in H9c2 rat ventricular cells. Control cells were mock-treated with lipofectamine 2000 for experiments involving transfection of dODN-NFAT or siRNAs. Note that NFAT does not affect miR-1 level. n=3 for INCA group and n=4 for the other groups.

## Supplemental Figure 14



**Supplemental Figure 14.** A. AF incidence in 1-week and 6-week atrial tachypacing (ATP) canine model. B. AF duration in ATP canine model. C. Quantitative RT-PCR measurement of miR-26a in atrium and ventricle of 1-wk and 6-wk ATP dogs. D. Western blot analysis of Kir2.1 protein in atrium and ventricle of 1-wk and 6-wk ATP dogs. n=5/group; \* $p$ <0.05, \*\* $p$ <0.01, \*\*\* $p$ <0.001.

**Supplemental Tables**

**Supplemental Table 1. Clinical characteristics of the patients used\* in our study**

<b>Patient No.</b>	<b>Gender</b>	<b>Age</b>	<b>Diagnosis</b>	<b>Surgery</b>
<b>Non-AF (NAF) Patients</b>				
NAF 1	male	43	Left atrial myxoma (SR)	Resection operation
NAF 2	male	52	CAD, Tricuspid incompetence. (SR)	TVP
NAF 3	female	46	RHD, MVS (SR)	MVR
NAF 4	female	22	CHD (SR)	CHD repair.
NAF 5	female	37	CAD, Tricuspid incompetence, Cardiac hypertrophy (SR)	TVP
NAF 6	male	55	Hypertension, MVP (SR)	MVR
NAF 7	male	44	Infective endocarditis (SR)	MVR
NAF 8	female	23	CHD (SR)	CHD repair.
NAF 9	male	30	Tricuspid incompetence (SR)	TVP
NAF 10	female	36	ASD (SR)	ASD closure.
<b>AF Patients</b>				
AF 1	male	39	RHD (AF)	AVR
AF 2	female	68	RHD, MVS (AF)	MVR, RFA

AF 3	male	55	MVD, AF	MVR, RFA
AF 4	female	56	CAD, AVS (AF)	AVR
AF 5	male	52	RHD (AF)	MVR, RFA
AF 6	female	56	RHD (AF)	MVR
AF 7	female	55	RHD, MVS (AF)	MVR, RFA
AF 8	female	66	RHD, MVS (AF)	MVR, RFA
AF 9	female	50	RHD, MVD (AF)	MVR, RFA
AF 10	female	59	RHD, MVD (AF)	MVR, RFA
AF 11	male	57	RHD, MVD (AF)	MVR, RFA
AF 12	female	54	RHD, MVD (AF)	MVR, RFA

\*Samples from a total of 22 patients were obtained (10 SR, 12 AF). Of these, 10 (NAF 1-5 and AF 1-5) were used for miRNA expression characterization; 11 (NAF 2-5, 6 and 7; AF 4, 6-9) were used for *KCNJ2* mRNA/protein expression measurement; 6 (NAF 8-10; AF 10-12) were used for immunohistochemical analyses of NFAT translocation.

Abbreviations: AF, atrial fibrillation; ASD, atrial septal defect; AVR, aortic valve replacement; AVS, aortic valve stenosis; CAD, coronary artery disease; CHD, congenital heart disease; MVP, mitral valve prolapse; MVR, mitral valve replacement; MVD, mitral valve disease; MVS, mitral valve stenosis; RFA, radiofrequency ablation; RHD, rheumatic heart disease; SR, sinus rhythm; TVP, tricuspid valvuloplasty.

**Supplemental Table 2. Echocardiographic data for mice subjected to miR-26a overexpression or knockdown**

	WT	Adv-miR-26a	Adv-miR-Free	LNA-antimiR-26a	MM LNA-antimiR-26a
BW (g)	29.87±0.81	29.66±1.11	29.18±0.69	29.87±0.81	28.42±0.44
HW (g)	0.13±0.01	0.13±0.01	0.13±0.002	0.12±0.004	0.12±0.003
HW/BW (mg/g)	4.21±0.18	4.37±0.17	4.40±0.10	4.15±0.12	4.29±0.10
LAID (cm)	0.20±0.01	0.20±0.02	0.21±0.01	0.20±0.01	0.21±0.01
IVSd (cm)	0.10±0.01	0.09±0.01	0.10±0.01	0.10±0.003	0.11±0.003
IVSs (cm)	0.12±0.003	0.13±0.01	0.14±0.01	0.13±0.01	0.12±0.005
LVIDd (cm)	0.33±0.01	0.32±0.02	0.37±0.02	0.35±0.02	0.30±0.01
LVIDs (cm)	0.21±0.01	0.21±0.03	0.24±0.02	0.22±0.01	0.20±0.01
LVPWd (cm)	0.11±0.01	0.09±0.01	0.09±0.005	0.11±0.01	0.11±0.01
LVPWs (cm)	0.11±0.01	0.09±0.01	0.11±0.01	0.12±0.01	0.13±0.01
EDV (ml)	0.09±0.01	0.09±0.01	0.14±0.02	0.11±0.02	0.08±0.01
ESV (ml)	0.03±0.01	0.03±0.01	0.04±0.01	0.03±0.03	0.02±0.003
EF (%)	70.0±6.0	68.9±7.5	70.5±3.0	71.3±1.9	68.9±4.6
SV (ml)	0.07±0.01	0.06±0.01	0.09±0.01	0.08±0.01	0.05±0.01
FS (%)	35.4±4.4	35.4±5.7	34.8±2.1	35.2±1.5	34.0±3.6

BW(g): Body Weight; HW(g): Heart Weight; LAID(cm): Left Atrial Internal Diameter; IVSd(cm): Interventricular Septum thickness at end-diastole; IVSs(cm): Interventricular Septum thickness at end-systolic; LVIDd(cm): Left Ventricular Internal Diameter at end-diastole; LVIDs(cm): Left Ventricular Internal Diameter at end-systolic; LVPWd(cm): LV Posterior Wall thickness in diastole; LVPWs(cm): LV Posterior Wall thickness in systolic; EDV(ml): End Diastolic Volume; ESV(ml): End Systolic Volume; EF(%): Ejection Fraction; SV (ml): Stroke Volume; FS(%): Fractional Shortening. n=5 per group; Data are mean ± SEM.

**Supplemental Table 3. Effects of miR-26a manipulation on electrophysiological parameters of mice**

	QTc Interval (ms)	QRS Duration (ms)	P-R Interval (ms)
Control/WT	49.4±1.5	9.3±0.5	45.7±2.2
Adv-miR-26a	56.3±2.1*	10.8±0.7	49.1±1.1
Adv-miR-Free	47.8±1.7	9.8±0.5	46.9±1.8
LNA-antimiR-26a	42.8±1.4*	9.8±0.6	45.4±1.2
MM LNA-antimiR-26a	49.2±2.2	9.4±0.5	47.5±1.5
Adv-miR-26a + miR-Mask	48.2±1.9†	9.4±0.5	47.1±2.1
LNA-antimiR-26a + miR-Mimic	48.5±1.4¶	9.5±0.4	46.8±1.9

Adv-miR-26a: adenovirus vector carrying pre-miR-26a; Adv-miR-Free: empty adenovirus vector; MM LNA-antimiR-26a: mismatched LNA-antimiR-26a; MM LNA-antimiR-1: mismatched LNA-antimiR-1; P-R interval: indicating atrioventricular conduction, mainly determined by L-type Ca<sup>2+</sup> current; QRS complex: indicating the excitation conduction time in ventricular tissues, mainly determined by Na<sup>+</sup> current; QTc: heart rate-corrected QT interval; Ctl/WT: control (wild-type) mice without gene-transfer.. \**p*<0.05 vs Control/WT; †*p*<0.05 vs Adv-miR-26a; ¶*p*<0.05 vs LNA-antimiR-26a; Student *t*-test; n=12 mice per group.

**Supplemental Table 4. Predicted NFAT binding motifs in the promoter regions of the host genes for the miR-26 family miRNAs of various species**

miRNA	Human	Canine	Rat	Mouse
<b>Host gene</b>	<b>Ctdspl; Chr3</b>	<b>Ctdspl; Chr23</b>	<b>Ctdspl; Chr8</b>	<b>Ctdspl; Chr9</b>
<b>miR-26a-1</b>	4430-GTGATGGAAACATTTGGAG (1/0.97)	2922-GCGGAGGAAAAAGTAGCTG (1/0.99)	2651-TATGGAAAGCTTAACTCTG (1/0.89)	2480-GTTGGAAATATCACCTGTT (1/0.89)
<b>NFAT Binding Sites</b>	†4040-ATGGAGGAAATTAGAGATG (1/1) ‡ 3992-CAGGTGGAAAGGCACTCCA (1/0.95) <b>3340-CATGAGGAAAAATATATC</b> (1/0.96)	1590-GCTGAGGAAATAAAGTAGG (1/1) 1479-CCTCAGGAAACAGTGGTCA (1/0.95) 1173-CACGGAAATTCACATGAAA (1/0.88)	2466-TTTGGAAACAGGCCACTC (1/0.87) 2285-AGAGGAAAGAGAATGGCTG (1/0.87) 2283-GGAGAGGAAAGAGAATGGC (1/0.99)	1293-GTTGGAAAGAACTTCCAG (1/0.88) 1213-CGTGGAAAAGTAAGGAAGT (1/0.92) 59-AAGGAGGAAAGCGAGGAGG (1/0.97)
<b>Host Gene</b>	<b>Ctdsp2; Chr12</b>	<b>Ctdsp2; Chr10</b>		<b>Ctdsp2; Chr10</b>
<b>miR-26a-2</b>	4480-TTGGAGGAAAGGAGAATGA (1/0.97)	2529-GTTGGAAACAGGGAAGCCT (1/0.99)		2507-GGGGGAAAAAGACAGGGTG (1/0.85)
<b>NFAT Binding Sites</b>	<b>3618-CCAGAGGAAAGGGGATACA</b> (1/0.97) 3385-CTATAGGAAAGAGGCCAC (1/0.96) 3361-TCTGGAAAGCTCTGTAGGG (1/0.92)			1535-GAAGAGGAAATGAACAGGA (1/0.97) 1177-AGGGGAAAAAGAGCAGTG (1/0.83) 304-GTCGGAAACACAAACACCC (1/0.83)
<b>Host Gene</b>	<b>Ctdsp1; Chr2</b>	<b>Ctdsp1; Chr37</b>	<b>Ctdsp1; Chr9</b>	<b>Ctdsp1; Chr1</b>
<b>miR-26b</b>	1134-GGAGAGGAAAGCGGCCAC (1/0.97)	209-GGGGAGGAAACTCCATGTT (1/0.97)	2999-TTTAAGGAAAGAGGCCAC (1/0.98)	2751-TTTAAGGAAAGAGGCCTAC (1/0.98)
<b>NFAT Binding Sites</b>	<b>373-AACGAGGAAAAAGACCAAC</b> (1/0.99) 371-AACGAGGAAACCGAGAAGC (1/0.84)	190-GCGGAGGAAACTTTGTAC (1/0.97)	2557-TGTGAGGAAACAAACAAAC (1/1) 107-GGGGAGGAAACTCCATGTT (1/0.97) 88-GCGGAGGAAACTTTGTAC (1/0.97)	2271-TGCAAGGAAACAAACAAAC (1/0.96) 1454-ACAGGAAAAATAAAAAATA (1/0.88) 434-GCTGGAAAAATGGCTCAGG (1/0.92)

Ctdsp: carboxy-terminal domain RNA polymerase II polypeptide A small phosphatase; Chr: chromosome; †The numbers before the sequences indicate the relative positions of the putative NFAT binding sites in the genome. ‡The numbers in the brackets indicate the scores for similarity of the putative NFAT *cis*-acting elements in the promoter regions of the host genes for the miR-26 family miRNAs to the canonical core binding sites and overall matrix for NFAT action, respectively; the sequences highlighted in yellow with boldface are the ones used for EMSA experiments.

**Supplemental Table 5. The primers used for PCR-amplification of miR-26 promoter sequences spanning NFAT *cis*-elements for chromatin immunoprecipitation assay (ChIP)**

<b>Host Gene /miRNA</b>	<b>Forward Primer</b>	<b>Reverse Primer</b>
<b>Ctdsp1/miR-26a-1</b>	5' -AAGTTTTTGTCACTCTCAGG-3'	5' -GTACCTATCCATGAGGAAAA-3'
<b>Ctdsp2/miR-26a-2</b>	5' -GGGGTAATGGGGACACTGCT-3'	5' -GGAGATAGCTGAAGCCAGGT-3'
<b>Ctdsp1/miR-26b</b>	5' -GCTCTTGACGTCCTTGCGAG-3'	5' -GGCTCCACCTCTGCGTTTTTC-3'

**Supplemental Table 6. The gene-specific primers (GSP) used for 5'RACE to identify the transcription start sites of the host genes for miR-26 miRNA family members**

<b>Host Gene /miRNA</b>	<b>GSP1 (Outer)</b>	<b>GSP2 (Nested)</b>
<b>Ctdspl/miR-26a-1</b>	5' -GCAACCGGCCCTCGTCCTCCT-3' (40 bp downstream of ATG)	5' -CTCGTCCTCCTTGGGGTTGGTC-3' (30 bp downstream of ATG)
<b>Ctdsp1/miR-26b</b>	5' -GAGGGAGGGGGCGCGGAGGA-3' (161 bp upstream to ATG)	5' -GGCGCGGAGGAACTTTG-3' (170 bp upstream to ATG)
<b>Ctdsp2/miR-26a-2</b>	5' -CCTCCCGGCTCTCGACTC-3' (387 bp upstream to ATG)	5' -TCTCGACTCGGCCTTTCAC-3' (396 bp upstream to ATG)

“ATG” indicates translational start site of the host genes.